

Quadratic Programming and Impedance Control for Transfemoral Prosthesis

Huihua Zhao, Shishir Kolathaya and Aaron D. Ames

Abstract—This paper presents a novel optimal control strategy combining control Lyapunov function (CLF) based quadratic programs with impedance control, with the goal of improving both tracking performance and the stability of controllers implemented on transfemoral prosthesis. CLF based quadratic programs have the inherent capacity to optimally track a desired trajectory. This property is used in congruence with impedance control—implemented as a feed-forward term—to realize significantly small tracking errors, while simultaneously yielding bipedal walking that is both stable and robust to disturbances. Moreover, instead of experimentally validating this on human subjects, a virtual prosthesis is attached to a robotic testbed, AMBER. The authors claim that the walking of AMBER is human like and therefore form a suitable substitute to human subjects on which a prosthetic control can be tested. Based on this idea, the proposed controller was first verified in simulation, then tested on the physical robot AMBER. The results indicate improved tracking performance, stability, and robustness to unknown disturbances.

I. INTRODUCTION

As one of the most important applications of bipedal robotic research, the development of lower-limb prosthetic devices and controllers for these devices has garnered the attention of the control and robotics communities in recent years [10], [17], [23], [24]. Different control strategies have been utilized for the control of transtibial and transfemoral prosthetic devices. Control based on gait-pattern generators has been considered in [19], [13]. Motion intent recognition with position control has been used in [10]. With the assumption that human gait is cyclical, impedance control is also one of the common approaches [9], [11], [23].

Inspired by the large body of work related to bipedal robotic locomotion and control implementation on prosthesis, there are three basic biomechanical requirements that must be satisfied for a transtibial or transfemoral prosthesis [20], [25]: (1) the prosthetic device must support the body weight of the amputee during the stance phase, i.e., the prosthesis control should provide “stability” during the weight bearing phase; (2) the physical interface between the able body and the prosthesis must prevent undesirable pressure during the locomotion. That is to say, the prosthetic controller must be “torque” optimal for the amputees wearing the device; (3) the prosthesis has to duplicate as nearly as possible the kinematics and dynamics of the normal gait. The amputee should be able to walk with normal appearance as the healthy people do.

The main results of this paper aim to address requirements (1) and (3) indicated above; this is achieved through two novel contributions. First, we introduce the idea of using bipedal robots to test prosthetic controllers—a nominal walking gait is found for the robot that is human-like, and prosthetic controllers are tested on a “leg” of the robot. Through this method, we are able to present and test a novel transfemoral prosthesis control method: control Lyapunov function (CLF) based quadratic programs (QPs) coupled with impedance control. In particular, we present a Model Independent QP (MIQP) utilizing CLFs to generate the feedback component of the controller and leverage impedance control to generate a robust feed-forward term. In addition, an impedance parameter estimation algorithm is also considered in this paper. With the proposed algorithm, we show that the estimated parameters from simulation can be directly applied experimentally with minimum parameter tuning (based upon hardware limitations of the platform being considered).

Before introducing our novel prosthetic control strategy—CLF based MIQP—we will first present one of the two major novel aspects of this paper: a method for testing prosthetic controllers via bipedal robots that display human-like locomotion. This allows for the collection of useful information regarding the performance of prosthetic control strategies to be gathered from the robot without the need for evasive tests on an amputee. Guided by this idea, the control strategy can be first designed and verified in simulation. With the model information of the physical robot, the essential control parameters can also be learned through simulation [3]. Then, a physical robot that has been shown to display qualitatively human-like walking, “wearing” a prosthetic device, can be used as a platform to test and polish the design of both the prosthesis controller and prosthetic device.

With the idea of using robot as the test platform for prosthetic control, we first show that we are able to achieve robot walking with prosthetic device using impedance control in both simulation and experiment. Based loosely on the definition of the impedance control, first proposed by Hogan [14], the torque at each joint during a single step cycle can be represented by a series of passive impedance functions [23]. By reproducing this torque at the prosthetic device joint using the passive impedance functions, one can obtain similar prosthetic gait compared to those found in normal gait tests. Normally, hand tuning from an expert is required to obtain the impedance parameters [8], [18], which, therefore, leads to another disadvantage—it is not optimal, i.e., when the prosthesis is off the designed trajectory, it may generate large torque while driving the device back to the equilibrium

*This research is supported by NASA grant NNX11AN06H, NSF grants CNS-0953823 and CNS-1136104.

H. Zhao, S. Kolathaya and A. Ames are with the department of Mechanical Engineering, Texas A & M University, 3128 TAMU, College Station, USA huihuazhao, shishirny, aames@tamu.edu

point. Considering all the drawbacks of impedance control, the obtained tracking performance is lacking, resulting in walking that is not as robust as desired.

Utilizing the impedance controller as a feed-forward term, we present a novel control method that will be utilized for feedback to increase robustness and stability. In particular, we begin by considering rapidly exponentially stabilizing control Lyapunov functions (RES-CLFs) as introduced in [6]. This class of CLFs can naturally be stated as inequality constraints in torque such that, when satisfied, rapid exponential convergence of the error is formally guaranteed. Furthermore, these inequality constraints can naturally be solved in an optimal fashion through the use of quadratic programs. The end result is a CLF based QP. Finally, due to the special structure of the RES-CLFs that will be considered in this paper, the CLF based QP can be stated in a model independent fashion. The end result is a novel feedback control methodology: Model Independent Quadratic Programs (MIQP) based upon RES-CLFs. These are combined with impedance control to obtain the final prosthetic controller. With the proposed controller, we will show that the tracking performance can be improved in both simulation and experiment. In addition, utilizing this novel control method, the robot displays improved stability and robustness to unknown disturbances.

The structure of this work is as following. Both the mathematical modeling of a hybrid system and the experiment model are introduced in Sec. II. The controller constructions of the impedance control and the CLF based MIQP control will be discussed in detail in Sec. III. Simulation results, including robustness tests by using different controllers will be showed in Sec. IV. Finally, the experimental results are presented on Sec. V. A video with details of both simulation and experiment results is attached at the end. Discussion and future work will be covered in Sec. VI.

II. ROBOT MODEL

In this section, we will start with a short description about the mathematical modeling of the hybrid bipedal robot. The physical robot, AMBER, which will be used as the test platform, is introduced at the end.

A. Robotic Model

The walking of bipedal robot displays both continuous behavior when the leg swings forward and discrete behavior when the swing foot hits the ground. Formally, we represent the bipedal robot considered in this paper as a hybrid system (see [4], [12] for a formal definition).

Continuous Dynamics. The configuration space of the robot \mathcal{Q}_R is described in body coordinates as: $\theta = (\theta_{sf}, \theta_{sk}, \theta_{sh}, \theta_{nsh}, \theta_{nsk})^T \in \mathbb{R}^5$, and the definition of each angle can be seen in Fig. 1. With the mass and length properties corresponding to the physical robot AMBER (see [26]), the equations of motion of the robot are given using the Euler-Lagrange formula:

$$D(\theta)\ddot{\theta} + H(\theta, \dot{\theta}) = Bu, \quad (1)$$

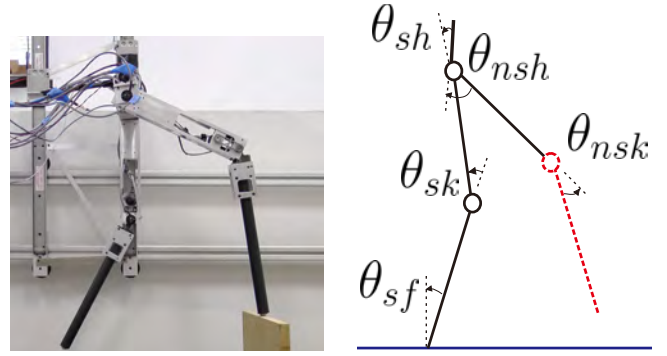


Fig. 1: The biped robot AMBER (left) and the angle conventions (right). The right leg with red dash line denotes the prosthetic device; the red dash circle represents the prosthetic joint that will be controlled using prosthetic controller.

where $D(\theta) \in \mathbb{R}^{5 \times 5}$ is the inertial matrix including the inertia of the boom, $B \in \mathbb{R}^{5 \times 4}$ is the torque map with the consideration of underactuation, and the control, u , is the vector of torque inputs. Note that, since AMBER has DC motors with small inductances, we can realize the electromechanical system with voltage inputs which have the following form:

$$V_{in} = R_a i_a + K_\omega \omega, \quad (2)$$

where V_{in} is the vector of voltage inputs to the motors, i_a is the vector of currents through the motors, R_a is the resistance matrix, and ω is the motor speed which has the relation as $\omega = r_m \dot{\theta}$ with r_m denoting the total reduction of the system. Since the motors are controlled individually, with the torque constant K_ϕ , the applied torques are:

$$u = K_\phi R_a^{-1} (V_{in} - K_\omega \omega). \quad (3)$$

Thus, the Euler-Lagrange equation can be reformulated as:

$$D(\theta)\ddot{\theta} + H_v(\theta, \dot{\theta}) = B_v V_{in}, \quad (4)$$

where $H_v(\theta, \dot{\theta}) = H(\theta, \dot{\theta}) + K_\phi R_a^{-1} K_\omega \omega$ and $B_v = B K_\phi R_a^{-1}$. Manipulation of (4) yields the affine control system (f, g) , details of which can be found to [4].

Discrete Dynamics. A discrete impact occurs instantaneously when the swing foot hits the ground. As a result, the velocities of the robot will change, combining with a leg switch simultaneously. Impacts are assumed to be perfect plastic impact as in [15], and the resulting reset map Δ_R is:

$$\Delta_R(\theta, \dot{\theta}) = \begin{bmatrix} \Delta_\theta \theta \\ \Delta_{\dot{\theta}}(\theta) \dot{\theta} \end{bmatrix}, \quad (5)$$

where Δ_θ is the relabeling which switches the stance and non-stance leg at impact, and $\Delta_{\dot{\theta}}$ determines the change in velocities due to the impact (see [4] for more details).

B. AMBER Test Platform

AMBER (short for A & M Bipedal Experimental Robot) is a planar bipedal robot with 5 links (one torso, two thighs and two calves, see Fig. 1). With pointed feet configuration, AMBER is powered only by 4 DC motors and is thus

underactuated at the ankles. Applying the human-inspired voltage controller, AMBER has achieved stable and human-like walking in experiment [26]. In this work, we use AMBER as the platform to test the proposed prosthetic controller. The right calf is assumed to be the “prosthetic device” which has the same length and mass configuration of the left calf which is marked as “healthy leg”. This assumption is reasonable, since it is essential to design a prosthetic device that has the mass and length properties similar to those of the amputee. The proposed controller will be used on the prosthetic device, i.e., on the right knee joint. The controller for the remaining actuations will still use the original P controller discussed in [26].

III. CONTROLLER CONSTRUCTION

In this section, we will introduce the idea of impedance controller briefly and extend the torque impedance to the voltage impedance to accommodate the control of AMBER. The algorithm of impedance parameter estimation will be discussed to obtain the impedance parameters automatically. Due to the shortcomings in impedance control, we propose the innovative CLF [5] based *model independent quadratic programming* (MIQP) control as the feedback term while using the impedance control as the feed-forward input.

A. Impedance Control for Prosthesis

We will now introduce the architecture of impedance control and then extend it for the voltage control of AMBER. The impedance parameter estimation algorithm will be presented at the end.

Impedance Control. Based on the notion of impedance control first proposed by Hogan [14], the torque at each joint during a single step can be piecewisely represented by a series of passive impedance functions [23] with the form:

$$\tau = k(\theta - q^e) + b\dot{\theta}. \quad (6)$$

where, k , q^e and b represent the stiffness, equilibrium angle and damping respectively, which are constant for specific sub-phase. This formula only requires local information about the controlled prosthetic joint—in this case the right knee joint (θ_{RK} , $\dot{\theta}_{RK}$)—so the end result is a simple prosthesis control. In particular, since the direct control input is voltage in AMBER, we can represent the joint input voltage during a single step by this function piecewisely with the form:

$$V^{imp} = k(\theta - q^e) + b\dot{\theta}, \quad (7)$$

where V^{imp} is termed as impedance voltage, which will be used as the control input of the prosthesis joint.

Phase Separation. While impedance control with a finite state machine is one of the most widely used algorithms suggested to date [16], one main problem is to identify the sub-phases correctly during a single step.

Based on the previous work [3], even though a point feet model is considered, analysis of AMBER walking data shows that one gait cycle can be divided into four phases based on the prosthesis knee joint, which are denoted as $p = 1, 2, 3, 4$,

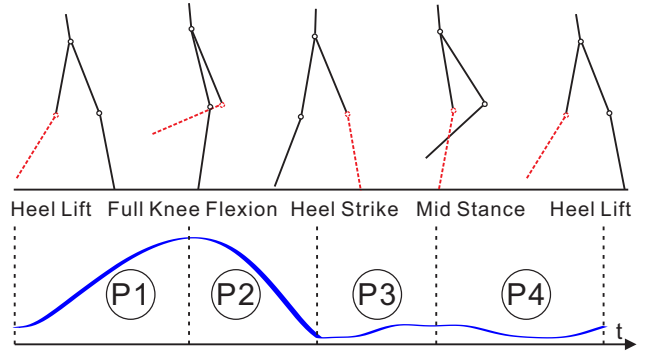


Fig. 2: AMBER gait phase separation. The red line represents the prosthetic device and the solid lines denote the able body. The green line is the knee angle of one full gait cycle.

as shown in Fig. 2. Specifically, each phase begins at time t_0^p and ends at t_f^p . The phase separation principle is similar as that in [3] but with values specific to the gait of AMBER. The impedance voltage at the prosthetic device (which is the right knee joint in this framework) during a phase $p \in \{1, 2, 3, 4\}$, can be represented by the following equation:

$$V_p^{imp} = k_p(\theta_{RK}(t) - q_p^e) + b_p\dot{\theta}_{RK}(t), \quad (8)$$

where $\theta_{RK}(t)$ and $\dot{\theta}_{RK}(t)$ denote angle and angular velocity of the right knee at time t . Therefore, in each phase p , the dynamics of the biped system is governed by the following Euler-Lagrange equation:

$$\begin{cases} D(\theta)\ddot{\theta} + H_v(\theta, \dot{\theta}) = B_v V_{in} & \forall t \in [t_0^p, t_f^p], \\ (\theta(t_0^p), \dot{\theta}(t_0^p)) = R(\theta(t_f^{p-1}), \dot{\theta}(t_f^{p-1})). \end{cases} \quad (9)$$

where $p-1 = 4$ if $p = 1$ and the switching function R has been defined as following:

$$R(\theta(t), \dot{\theta}(t)) = \begin{cases} \Delta(\theta(t), \dot{\theta}(t)) & \text{at impacts,} \\ (\theta(t), \dot{\theta}(t)) & \text{otherwise.} \end{cases} \quad (10)$$

Specifically, for the prosthesis joint, we will replace the corresponding V_{in} term with the prosthetic voltage input V_p^{imp} , which yields the following set up:

$$D^i(\theta)\ddot{\theta} + H_v^i(\theta, \dot{\theta}) = B_v^i V_p^{imp} \quad \forall t \in [t_0^p, t_f^p], \quad (11)$$

where i indicates the i th row of the corresponding term, which will be updated according to the sub-phase p . Note that, since we define the body coordinates based on the stance and non-stance nomenclature, we have $i = 5$ when $p = 1, 2$, i.e., the prosthetic device is the non-stance leg, and $i = 2$ while $p = 3, 4$, i.e., the prosthetic device is the swing leg.

Impedance Parameter Estimation. With the phase transitions defined above, another problem of impedance control is to identify the control parameters for each sub-phase. Learning parameters can be a tedious job requiring hand tuning by an expert [8], [18]. Moreover, this method can be especially expensive when it is extended to learning controller parameters for a specific amputee subject.

In the previous work [3], the authors showed that the impedance parameters for a lower-limb prosthesis can be

learned by the observation of unimpaired human walkers. The results have been validated both in simulation and in an experiment with a transfemoral prosthetic device. To extend these results, we utilize a similar method to estimate the impedance parameters by observing the simulated “unimpaired” walking data of AMBER.

We first define the impedance parameter set as $\beta_p = \{k_p, b_p, q_p^e\}$ for specific sub-phase p . With the walking data $x = (\theta, \dot{\theta})^T$ and V_{RK} obtained by utilizing the human-inspired voltage P controller on AMBER in simulation, we can form the least square errors minimization problem as following:

$$\beta_p^* = \operatorname{argmin}_{\beta_p} \int_{t_0^p}^{t_f^p} (V_p^{imp} - V_{RK,p})^2 dt, \quad (12)$$

where V_p^{imp} is defined as (8) and $V_{RK,p}$ is the “healthy” input voltage on the right knee joint at sub-phase p . By solving this minimization problem, the estimated impedance parameters for each sub-phase can be seen in Table. I.

B. CLF Model Independent QP

With the specifically defined human-inspired constraints obtained by looking at human locomotion data, human-inspired controller has been applied successfully to achieve walking on both fully and under actuated physical robots [21], [26]. In this section, the brief revisit of the human-inspired control will be given first (the detailed work can be referred to [4], [22]). Based on this foundational work and inspired by the CLF controller in [5], we will discuss the novel CLF based model independent control in detail.

Human-Inspired Control Revisit. Motivated by the goal of achieving human-like bipedal robotic walking, human-inspired controller aims to drive the actual robot outputs $y_a(\theta)$, which are joint angles or functions of joint angles, to the desired human outputs $y_d(t, \alpha)$ which can be represented by the CWF introduced in [4]. Therefore, motivating the introduction of human-inspired outputs, we have:

$$y(\theta, \dot{\theta}) = \begin{bmatrix} y_1(\theta, \dot{\theta}) \\ y_2(\theta) \end{bmatrix} = \begin{bmatrix} y_1^a(\theta, \dot{\theta}) - v_{hip} \\ y_2^a(\theta) - y_2^d(\tau(\theta), \alpha) \end{bmatrix}, \quad (13)$$

where $y_1(\theta, \dot{\theta})$ is the relative degree one output, which is the difference between the actual forward hip velocity $y_1^a(\theta, \dot{\theta})$ and the desired hip velocity v_{hip} . And $y_2(\theta)$ are the relative degree two human-inspired outputs which are the difference between the actual relative degree two outputs $y_2^a(\theta)$ which are both the knee angles and the hip angle (see [4] for more details), and the desired relative degree two outputs $y_2^d(\theta)$.

With this construction in hand, we can represent the dynamics in (4) in outputs space by differentiating the $y(\theta, \dot{\theta})$:

$$\begin{bmatrix} \dot{y}_1 \\ \dot{y}_2 \end{bmatrix} = \underbrace{\begin{bmatrix} L_f y_1(\theta, \dot{\theta}) \\ L_f^2 y_2(\theta, \dot{\theta}) \end{bmatrix}}_{L_f} + \underbrace{\begin{bmatrix} L_g y_1(\theta, \dot{\theta}) \\ L_g L_f y_2(\theta, \dot{\theta}) \end{bmatrix}}_A u \quad (14)$$

where L_f is the Lie derivative and A is dynamic decoupling matrix, which is nonlinear most of the cases. By picking:

$$u = A^{-1}(L_f + \mu), \quad (15)$$

the equation (14) turns into the linear form:

$$\begin{bmatrix} \dot{y}_1 \\ \dot{y}_2 \end{bmatrix} = \mu. \quad (16)$$

By designing μ properly, [4] for example, one can drive both $y_1 \rightarrow 0$ and $y_2 \rightarrow 0$ exponentially; therefore, human-inspired walking has been achieved.

This control strategy works for nonlinear systems, but requires a good knowledge about the model. In the domain of complex nonlinear robotic control, this assumption is usually not satisfied, which renders the computed torque to be far away from the required torque. PID control still dominates in real world control problems since it doesn't require accurate model information, i.e., it is model independent. However, considering all the well-known problems of PID control (hand tuning, none optimal [7]), we are motivated to find a new optimal control strategy to overcome these issues while maintaining the model insensitive property. With the framework of human-inspired control, an optimal model independent control will be introduced in the following.

CLF MIQP. With defining the vector $\eta = (y, \dot{y})^T \in \mathbb{R}^{2 \times 1}$ since only the knee joint is considered, the equation (16) can be rewritten as a linear control system:

$$\eta = \underbrace{\begin{bmatrix} 0 & 1 \\ 0 & 0 \end{bmatrix}}_F \eta + \underbrace{\begin{bmatrix} 0 \\ 1 \end{bmatrix}}_G \mu. \quad (17)$$

In the context of this control system, we consider the continuous time algebraic Riccati equations (CARE):

$$F^T P + P F - 2 P G G^T P + I = 0, \quad (18)$$

where $P = P^T > 0$. With the optimal solution $\mu = -G^T P \eta$, we obtain the optimal control law that minimizes the cost:

$$\int_0^\infty (\eta^T \eta + \mu^T \mu) dt. \quad (19)$$

With the aim to have stronger bounds of the convergence of the considered hybrid system, we take this method further by defining $\eta_\varepsilon = (y/\varepsilon, \dot{y})^T$. Followed by that, we can choose P and $\varepsilon > 0$ carefully to construct a *rapidly exponentially stabilizing control Lyapunov function (RES-CLF)* that can be used to stabilize the output dynamics with a rapidly exponentially fashion (the detailed proof can be seen in [6]). In particular, we define the positive definite CLF as:

$$V_\varepsilon(\eta) = \eta^T \begin{bmatrix} \frac{1}{\varepsilon} I & 0 \\ 0 & I \end{bmatrix} P \begin{bmatrix} \frac{1}{\varepsilon} I & 0 \\ 0 & I \end{bmatrix} \eta := \eta^T P_\varepsilon \eta. \quad (20)$$

Differentiating this function renders:

$$\dot{V}_\varepsilon(\eta) = L_f V_\varepsilon(\eta) + L_g V_\varepsilon(\eta) \mu, \quad (21)$$

where $L_f V_\varepsilon(\eta) = \eta^T (F^T P_\varepsilon + P_\varepsilon F) \eta$, $L_g V_\varepsilon(\eta) = 2 \eta^T P_\varepsilon G$.

In order to exponentially stabilize the system, we want to find μ such that, for specifically picked $\gamma > 0$ [6], we have:

$$L_f V_\varepsilon(\eta) + L_g V_\varepsilon(\eta) \mu \leq -\frac{\gamma}{\varepsilon} V_\varepsilon(\eta). \quad (22)$$

Therefore, an optimal μ could be found by solving the following minimization problem:

$$m(\eta) = \operatorname{argmin}\{\|\mu\| : \varphi_0(\eta) + \varphi_1(\eta)\mu \leq 0.\}, \quad (23)$$

which is equivalent to solve the quadratic program (QP) as:

$$\begin{aligned} m(\eta) = \operatorname{argmin}_{\mu \in \mathbb{R}^{n_1+n_2}} \mu^T \mu & \quad (24) \\ \text{s.t } \varphi_0(\eta) + \varphi_1(\eta)\mu \leq 0, & \quad (\text{CLF}) \end{aligned}$$

where $\varphi_0(\eta) = L_f V_\varepsilon(\eta) + \frac{\gamma}{\varepsilon} V_\varepsilon(\eta)$ and $\varphi_1(\eta) = L_g V_\varepsilon(\eta)$. Note that, n_1, n_2 correspond to the relative degree one outputs and relative degree two outputs. In this case, we have $n_1 = 0$ and $n_2 = 1$ since we are only considering the knee joint.

Note that, instead of substituting the optimal solution μ into equation (15) to obtain the feedback control law as in [5], we use μ directly as control input into the original system without considering the model decoupling matrix A and L_f . Therefore, we term this strategy *Model Independent Quadratic Program* (MIQP) controller.

Taking a further look into the MIQP algorithm, we basically constructed a new linear control system (17) that only focuses on the errors between the actual outputs and desired outputs, while not requiring any information about the original model. Another immediate advantage is that the torque bounds can be directly applied in this formulation where, the optimal control value can be obtained while respecting the torque bounds. As discussed in [5], this can be achieved by relaxing the CLF constraints with a large penalty value $p > 0$. In particular, we consider the MIQP as:

$$\begin{aligned} \operatorname{argmin}_{(\delta, \mu) \in \mathbb{R}^{n_1+n_2+1}} p\delta^2 + \mu^T \mu & \quad (25) \\ \text{s.t } \varphi_0(\eta) + \varphi_1(\eta)\mu \leq \delta, & \quad (\text{CLF}) \\ \mu \leq \mu_{MAX}, & \quad (\text{Max Torque}) \\ -\mu \leq \mu_{MAX}. & \quad (\text{Min Torque}) \end{aligned}$$

Similarly, for the control of AMBER, the term μ can be replaced with the input voltage V_{in} directly without affecting the configuration of this algorithm.

MIQP + Impedance Control. Utilizing the formal framework discussed above, we are now ready to introduce another main result of this paper, which is the MIQP + Impedance controller for prosthesis.

While MIQP control benefits its model independent property with an optimal fashion in practical application, it also suffers the over shooting problem as the PID controller does. Particularly, over shooting issue will be a fatal problem for a prosthesis controller with the safety consideration of the amputee; therefore, this motivates the introduction of MIQP + Impedance control.

With the impedance control V^{imp} as the feed-forward term, the input voltage V_{in}^p of the prosthetic leg, or the system (17) can be stated as follows:

$$V_{in}^p = V^{qp} + V^{imp}, \quad (26)$$

where V^{qp} is the voltage computed from the MIQP problem. To take a further step, we add the impedance term V^{imp} into

the MIQP construction, which yields the following MIQP + Impedance problem:

$$\begin{aligned} \operatorname{argmin}_{(\delta, V^{qp}) \in \mathbb{R}^{n_1+n_2+1}} p\delta^2 + V^{qpT} V^{qp} & \quad (27) \\ \text{s.t } \varphi_0(\eta) + \varphi_1(\eta)V^{qp} \leq \delta + \varphi_1(\eta)V^{imp}, & \quad (\text{CLF}) \\ V^{qp} \leq V_{MAX}^{qp}, & \quad (\text{Max QP Voltage}) \\ -V^{qp} \leq V_{MAX}^{qp}, & \quad (\text{Min QP Voltage}) \\ V^{qp} \leq V_{MAX} - V^{imp}, & \quad (\text{Max Input Voltage}) \\ -V^{qp} \leq V_{MAX} + V^{imp}. & \quad (\text{Min Input Voltage}) \end{aligned}$$

By adding the impedance feed-forward term into the QP problem, the model independent outputs dynamic system (17) gathers information about the system that it is controlling, therefore we can adjust the V^{qp} accordingly to accommodate the feed-forward term in order to achieve exceptional tracking. By setting the QP voltage bounds V_{MAX}^{qp} , we can control the overshooting problem. Note that, we also set the total input voltage bounds for the QP problem such that the final total optimal input voltage (26) will satisfy the input voltage bounds which are constrained by the hardware.

To summarize, the MIQP + Impedance control method combines the advantages from both the impedance controller which is derived from the model and the MIQP controller that is optimal for tracking. Therefore, it will generate a better tracking performance due to the optimal nature of the controller while having better uncertainty tolerance and disturbance rejection properties. In the preceding sections, we will implement this controller in both simulation and experiment, and comparisons will be made between the other two control methods introduced.

IV. PROSTHETIC WALKING IN SIMULATION

With the control architecture in hand, the simulation results of the AMBER model will be discussed in this section. As discussed above, the right leg is assumed to be the prosthetic device, therefore, will be controlled with the independent prosthetic controller. The tracking results of the prosthesis joint by using different controllers will be compared. Finally, robustness tests will also be performed with the proposed MIQP + Impedance controller.

A. Tracking Performance with Different Controllers

With the exception of the prosthesis knee joint, on which we will use different controllers, the remaining joints will be controlled with the human-inspired voltage P control which has been presented in detail in [26]. Using the method discussed in Sec. III-A, the estimated impedance controller parameters from simulation are shown in Table I.

Three different controllers have been implemented as the prosthetic controller: P control, impedance control and MIQP + Impedance control. Fig. 6 shows the tracking performance of the prosthesis knee joint using these three different controllers. Using the tracking results of P control as a nominal reference (as shown in Fig. 6a), we can see that MIQP + Impedance control has improved the tracking performance in both stance phase and non-stance phase by more than 10

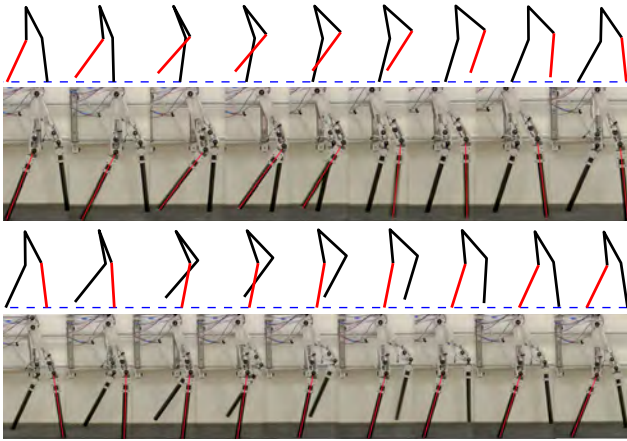


Fig. 3: Experimental and simulation gait tiles with only impedance controller. Red line indicates the prosthesis.

times w.r.t the *RMS* error, while impedance control yields tracking that is worse than the P control.

The gait tiles of two steps walking by using impedance control and MIQP + Impedance control can be seen in Fig. 3 and Fig. 4. Each of these shows good walking while the gait with impedance control tends to have bigger knee extension. Particularly, with impedance control, the robot can only walk 12 steps in simulation. This is reasonable since we consider underactuated ankles in this framework. Impedance control is fundamentally passive nature, and therefore cannot correct the tracking error efficiently; therefore, any small error in tracking will lead to a failure to walk. The phase portrait for 32 steps with using voltage P control can be seen in Fig. 7, which clearly shows the convergence to one periodic orbit since the controls are same on both the legs. The phase portrait for 64 steps with using MIQP + Impedance can be seen in Fig. 8, which shows that the phase portrait converges to two limit cycles since the controllers are asymmetric.

With the comparison above, we can conclude that MIQP + Impedance controller delivers improved tracking performance without increasing the torque requirement (due to the formulation of the MIQP algorithm), which is the key perspective while evaluating a prosthetic controller.

B. Stability Testing

Stability is another fundamental requirement for a prosthesis controller. With the proposed MIQP + Impedance method, we claim that this controller renders more robustness to the prosthetic device than only using impedance control, therefore, is safer for the amputee's daily use. In this section, two robustness tests will be applied to the robot in simulation; one is to add a instantaneous push to the robot and another one is to let the robot walk above an obstacle.

Reaction to impulse push. A $2N$ impulse force (lasting for $0.05s$) that equals about 10% of the total weight of AMBER, has been applied to the prosthetic leg while it's in the swing phase. From the video [1], we can see that the prosthetic device with the proposed controller can tolerate this disturbance and maintain good tracking. We also tested

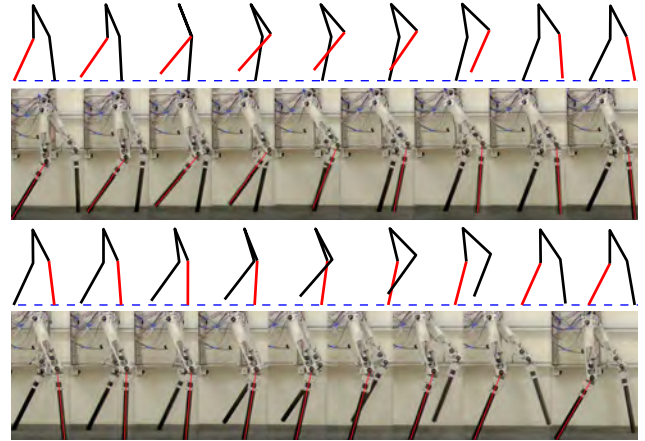


Fig. 4: Experimental and simulation gait tiles using MIQP + Impedance control. Red line indicates the prosthesis.

this disturbance with only impedance controller; the tracking error becomes bigger due to the disturbance and the robot falls after 6 steps.

To overcome an obstacle. In the simulation, we let the robot walk over a 20 mm obstacle. The gait tiles can be seen in Fig. 5, from which shows that the robot can overcome the obstacle smoothly. The results show that after walking over the obstacle, the robot can keep walking as normal and remaining good tracking. A similar test is also conducted with only impedance control. The robot can walk over the obstacle, however, the tracking performance becomes worse. Both the tests are shown in the video [1] with details.

V. EXPERIMENTAL IMPLEMENTATION AND RESULTS

After being verified in simulation, the controllers were tested on the physical robot AMBER. The right knee joint was considered to be the prosthetic joint and controlled with the prosthetic controller. In this section, the experimental setup and results will be presented.

A. Impedance Control

The final goal of the impedance parameter estimation idea is to use the estimated impedance parameters obtained from simulation directly in the physical robot such that no tuning is required. Starting with the estimated impedance parameters, we are able to tune the parameters within a small range and get sustainable walking by only using the

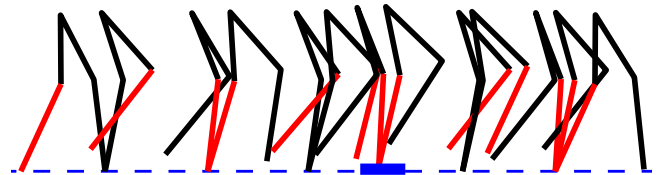


Fig. 5: Gait tiles of walking over an obstacle with MIQP + Impedance control.

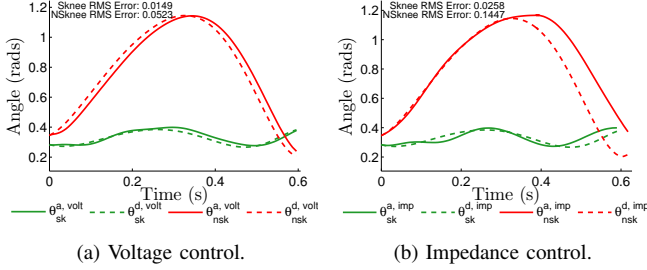


Fig. 6: Actual and desired outputs of the prosthesis knee joint with different controllers in simulation.

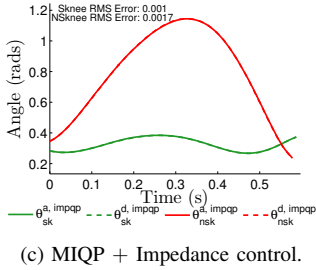


Fig. 7: Phase portrait of prosthesis joint with voltage control.

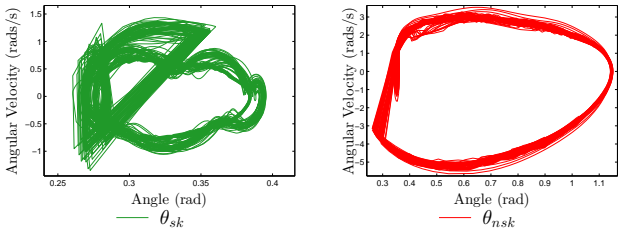


Fig. 8: Phase portrait of prosthesis joint with MIQP + Impedance control.

impedance controller. The actual impedance parameters used on the robot are shown in Table I. Note that, the actual k parameters are bigger than the estimated values and the b parameters are kept low. The main reasons are twofold. Firstly, in simulation, the friction and damping of the transmission, i.e., the motor and gear box, are not considered. Therefore, we need higher k parameters to compensate for the model differences. The second reason is that the angular velocity information from AMBER is not accurate, bordering being unusable, which prevents the use of the velocity terms. Therefore, b terms has to be lowered, which, as a result, leads

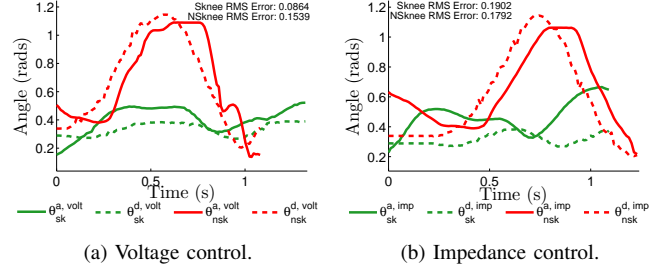
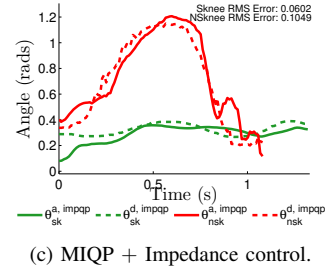


Fig. 9: Actual and desired outputs of the prosthesis knee joint with different controllers in experiment.



(c) MIQP + Impedance control.

to higher k parameters in order to provide enough torque.

Besides the discussions above, we claim that the estimated impedance parameters can capture the essentials of the physical model, thus the requirement of hand tuning can be kept to minimum. The tracking result of using impedance controller can be seen in Fig. 9b. Comparing to the tracking of P control as shown in Fig. 9a, the impedance control shows bad tracking performance. The experimental gait tiles are also compared side by side with the simulated gait tiles using only impedance control.

B. MIQP + Impedance Control

Using the same impedance parameters in Sec. V-A, we apply the impedance control as the feed-forward term while using the MIQP as the feedback term to correct the tracking errors and reject the disturbances. As discussed above, the velocity sensor data of AMBER is very noisy, therefore, only the position data is used for the MIQP algorithm, which we find to be sufficient in achieving good tracking. From the Fig. 9c, we can see the tracking with using MIQP + Impedance controller is the best among the three methods in both stance phase and non-stance phase (RMS error reduced by 50% for both phases). We also tested the robustness of the walking with MIQP + Impedance control, the robot was able to overcome a 40 mm block and could stand for big pushes on the prosthetic leg. The details can be seen in the video [1]. Note that, in the video, the walking gait using MIQP + Impedance control is not as smooth as that with using only voltage P control. Again, this is because of the fact that the prosthetic joint has better tracking than the healthy joint, therefore, the gait is asymmetric.

TABLE I: Impedance Parameters of the Prosthesis.

Sim/Exp	Estimated parameters			Experimental parameters		
Phase	k^p [V]	b^p [V·s]	q_e [rad]	k^p [V]	b^p [V·s]	q_e [rad]
P1	-3.9731	0.1242	0.2493	-12.9731	0.0242	0.1283
P2	-3.7714	0.1499	0.2327	-18.7714	0.0499	0.1
P3	-0.2123	0.1405	1.1378	-15.212	0.1405	1.1405
P4	-0.1956	0.1418	0.1999	-18.5568	0.0044	0.1024

VI. CONCLUSIONS AND FUTURE WORK

Two objectives have been achieved in this framework. First, we proposed a new method which is to test and design the prosthesis controllers on a robot (rather than an amputee) which has been shown to have qualitatively human-like walking obtained through the human-inspired controller [4]. Since the physical robot displays human-like walking gait, which captures the essentials of human locomotion, we claim that testing the prosthetic controller (or device) in such a robot will yield us qualitative information, and therefore, can help us improve the designs of both the prosthetic controller and the lower-limb prosthetic device. This method will save expenses and time resources of clinical experts and patients, and it will also relieve the pains of the amputee while testing a new prosthesis in the early stage.

Then, a novel optimal control algorithm: MIQP + Impedance control was introduced to control the prosthetic device using the framework discussed above. This controller benefits both the feed-forward impedance control that gives us model information and the MIQP method that renders model independent control in an optimal fashion that is inherited from the CLF based QP control method. This controller has been verified on robots using the idea discussed above in both simulation and experiment. Compared with the other two control methods, P controller and impedance controller, the proposed optimal controller shows the best tracking performance while using the same level of energy input. The robustness tests also show that this optimal controller can overcome disturbances and obstacles while displaying good tracking in both simulation and experiment.

Future Work. The limitations of this work are mainly due to the robot hardware. AMBER doesn't have feet and the ankle is underactuated. Also, the velocity sensor data is not usable, which limits the performance of the MIQP algorithm. In the future work, we are going to test the same algorithm on the footed robot AMBER2 which has achieved good human-like walking with both knee and ankle actuated, the video of which can be seen in [2].

REFERENCES

- [1] Experimental and simulation results. <http://youtu.be/5TuTyKhMniU>.
- [2] Sustainable walking of amber2. <http://youtu.be/d6oM5sLI9vA>.
- [3] Navid Aghasadeghi, Huihua Zhao, Levi J Hargrove, Aaron D Ames, Eric J Perreault, and Timothy Bretl. Learning impedance controller parameters for lower-limb prostheses. *IEEE: IROS*, 2013.
- [4] A. D. Ames. First steps toward automatically generating bipedal robotic walking from human data. In *8th International Workshop on Robotic Motion and Control, RoMoCo'11*, Bukowy Dworek, 2011.
- [5] Aaron D Ames. Human-inspired control of bipedal robots via control lyapunov functions and quadratic programs. In *Proceedings of the 16th international conference on Hybrid systems: computation and control*, pages 31–32. ACM, 2013.
- [6] A.D. Ames, K. Galloway, and J.W. Grizzle. Control lyapunov functions and hybrid zero dynamics. In *Decision and Control (CDC), 2012 IEEE 51st Annual Conference on*, pages 6837–6842, 2012.
- [7] D.P. Atherton and S. Majhi. Limitations of pid controllers. In *American Control Conference, 1999. Proceedings of the 1999*, pages 3843–3847, 1999.
- [8] Christopher G Atkeson and Stefan Schaal. Robot learning from demonstration. In *ICML*, volume 97, pages 12–20, 1997.
- [9] Samuel Au, Max Berniker, and Hugh Herr. Powered ankle-foot prosthesis to assist level-ground and stair-descent gaits. *Neural Networks*, 21(4):654 – 666, 2008. $\text{jce:title}_{\text{Robotics}}$ and Neuroscience ; $\text{ce:title}_{\text{}}$.
- [10] S.K. Au, P. Bonato, and H. Herr. An emg-position controlled system for an active ankle-foot prosthesis: an initial experimental study. In *Rehabilitation Robotics, 2005. ICORR 2005. 9th International Conference on*, pages 375–379, 2005.
- [11] J.A. Blaya and H. Herr. Adaptive control of a variable-impedance ankle-foot orthosis to assist drop-foot gait. *Neural Systems and Rehabilitation Engineering, IEEE Transactions on*, 12(1):24–31, 2004.
- [12] J. W. Grizzle, C. Chevallereau, A. D. Ames, and R. W. Sinnet. 3D bipedal robotic walking: models, feedback control, and open problems. In *IFAC Symposium on Nonlinear Control Systems*, Bologna, September 2010.
- [13] Joseph Hitt, A Mehmet Oymagil, Thomas Sugar, Kevin Hollander, Alex Boehler, and Jennifer Fleeger. Dynamically controlled ankle-foot orthosis (dco) with regenerative kinetics: incrementally attaining user portability. In *Robotics and Automation, 2007 IEEE International Conference on*, pages 1541–1546. IEEE, 2007.
- [14] Neville Hogan. Impedance control: An approach to manipulation. pages 304–313, 1984.
- [15] Y. Hürmüzülü and D. B. Marghitu. Rigid body collisions of planar kinematic chains with multiple contact points. *Intl. J. of Robotics Research*, 13(1):82–92, February 1994.
- [16] René Jimenez-Fabian and Olivier Verlinden. Review of control algorithms for robotic ankle systems in lower-limb orthoses, prostheses, and exoskeletons. *Medical engineering & physics*, 34(4):397–408.
- [17] EC Martinez-Villalpando. Design of an agonist-antagonist active knee prosthesis. . . ., 2008. *BioRob 2008*. . . ., pages 529–534, 2008.
- [18] Jun Nakanishi, Jun Morimoto, Gen Endo, Gordon Cheng, Stefan Schaal, and Mitsuo Kawato. Learning from demonstration and adaptation of biped locomotion. *Robotics and Autonomous Systems*, 47(2):79–91, 2004.
- [19] Aykut Mehmet Oymagil, Joseph K Hitt, Thomas Sugar, and Jennifer Fleeger. Control of a regenerative braking powered ankle foot orthosis. In *Rehabilitation Robotics, 2007. ICORR 2007. IEEE 10th International Conference on*, pages 28–34. IEEE, 2007.
- [20] Dejan Popovic, Rajko Tomovic, Dejan Tepavac, and Laszlo Schwirtlich. Control aspects of active above-knee prosthesis. *International Journal of Man-Machine Studies*, 35(6):751 – 767, 1991.
- [21] M Powell, Ayonga Hereid, and Aaron D Ames. Speed regulation in 3d robotic walking through motion transitions between human-inspired partial hybrid zero dynamics.
- [22] M.J. Powell, Huihua Zhao, and A.D. Ames. Motion primitives for human-inspired bipedal robotic locomotion: walking and stair climbing. In *Robotics and Automation (ICRA), 2012 IEEE International Conference on*, pages 543–549, 2012.
- [23] Frank Sup, Amit Bohara, and Michael Goldfarb. Design and Control of a Powered Transfemoral Prosthesis. *The International journal of robotics research*, 27(2):263–273, February 2008.
- [24] Frank Sup, Huseyin Atakan Varol, and Michael Goldfarb. Upslope walking with a powered knee and ankle prosthesis: initial results with an amputee subject. *IEEE transactions on neural systems and rehabilitation engineering : a publication of the IEEE Engineering in Medicine and Biology Society*, 19(1):71–8, February 2011.
- [25] Radcliffe C. W. Biomechanical basis for the design of prosthetic knee mechanisms. *Rehabilitation Engineering International Seminar REIS' 80*, 1980.
- [26] Shishir Nadubettu Yadukumar, Murali Pasupuleti, and Aaron D Ames. From formal methods to algorithmic implementation of human inspired control on bipedal robots. In *Algorithmic Foundations of Robotics X*, pages 511–526. Springer, 2013.